Research Square

Preprints are preliminary reports that have not undergone peer review.
They should not be considered conclusive, used to inform clinical practice,
or referenced by the media as validated information.

Socio-economic flood resilience reveals welfare-vulnerable communities obscured by asset-based appraisals

Jie Liu

liu_jie521188@163.com

University of Cambridge https://orcid.org/0000-0002-1920-1043

Junying Liu

Tianjin University

Tonglaga Wang

Tianjin University

Zhengyang Li

The Hong Kong Polytechnic University https://orcid.org/0000-0002-9208-0487

Zizhen Xu

University of Cambridge https://orcid.org/0000-0003-1808-1729

Oded Cats

Delft University of Technology

Gemma Cremen

University College London (UCL) https://orcid.org/0000-0002-6699-7312

Jiaoe Wang

Institute of Geographic Sciences and Natural Resources Research, Chinese Academy of Sciences
https://orcid.org/0000-0003-1051-7727

Mingwei He

Kunming University of Science and Technology

Anthony Chen

The Hong Kong Polytechnic University https://orcid.org/0000-0003-4363-5041

Stephanie Galaitisi

Engineer Research and Development Center

Igor Linkov

Carnegie Mellon University

Ramit Debnath

University of Cambridge https://orcid.org/0000-0003-0727-5683

Article

Keywords:

Posted Date: November 16th, 2026

DOI: https://doi.org/10.21203/rs.3.rs-11539385/v1

License: This work is licensed under a Creative Commons Attribution 4.0 International License.
Read Full License

Additional Declarations: Yes there is potential Competing Interest. Ramit Debnath is the guest editor for the Nature special collection on Managing cascading and non-linear climate risks. The other authors declare no competing interests.

Socio-economic flood resilience reveals welfare-vulnerable communities obscured by asset-based appraisals

Junying Liu[1,2]
[1] College of Management and Economics, Tianjin University, Tianjin, China
[2] Laboratory of Computation and Analytics of Complex Management Systems (CACMS), Tianjin University, Tianjin, China
Email: liujunying@tju.edu.cn

Tonglaga Wang[1]
[1] College of Management and Economics, Tianjin University, Tianjin, China
Email: wangtlg_2022@tju.edu.cn

Zhengyang Li[3]
[3] Department of Civil and Environmental Engineering, The Hong Kong Polytechnic University, Hong Kong, China
Email: zhengyang.li@connect.polyu.hk

Zizhen Xu[4]
[4] Department of Engineering, University of Cambridge, Cambridge, United Kingdom
Email: zx311@cam.ac.uk

Oded Cats[5]
[5] Department of Transport & Planning, Faculty of Civil Engineering and Geosciences, Delft University of Technology, Delft, Netherlands
Email: o.cats@tudelft.nl

Jie Liu[4,*]
[4] Department of Engineering, University of Cambridge, Cambridge, United Kingdom
Email: liu_jie521188@163.com; jl2439@cam.ac.uk

Gemma Cremen[6]
[6] Department of Civil, Environmental and Geomatic Engineering, University College London, London, United Kingdom
Email: g.cremen@ucl.ac.uk

Jiaoe Wang[7]

[7] Institute of Geographic Sciences and Natural Resources Research, Chinese Academy of Sciences, Beijing, China

Email: wangje@igsnrr.ac.cn

Mingwei He[8]

[8] Faculty of Transportation Engineering, Kunming University of Science and Technology, Kunming, China

Email: kmhmw@kust.edu.cn

Anthony Chen[3]

[3] Department of Civil and Environmental Engineering, The Hong Kong Polytechnic University, Hong Kong, China

Email: anthony.chen@polyu.edu.hk

Stephanie E. Galaitsi[9]

[9] Credere LLC, Westbrook, ME, USA

Email: stephanie.e.galaitsi@usace.army.mil

Igor Linkov[10]

[10] Carnegie Mellon University, Pittsburgh, PA, USA

Email: ilinkov@yahoo.com

Ramit Debnath[11,12]

[11] Centre for Human-Inspired AI, University of Cambridge, Cambridge, United Kingdom

[12] Linde Centre for Science, Society and Public Policy, California Institute of Technology, USA

Email: rd545@cam.ac.uk

Corresponding author: Jie Liu

Abstract

Asset-based flood risk assessments can obscure inequalities in welfare impacts. We integrate two-metre-resolution flood hazard maps, socioeconomic data and a dynamic recovery model to quantify socio-economic flood resilience (SEFR), defined as asset loss divided by monetised well-being loss. Analysis of 6,791 English neighbourhoods across flood sources and return periods under present-day and future RCP8.5 conditions reveals highly unequal household asset and well-being losses. More deprived neighbourhoods, characterised by social and economic disadvantage, consistently have lower SEFR, while low-SEFR neighbourhoods cluster spatially, revealing concentrated welfare vulnerability. These patterns produce divergent priorities: across flood scenarios, 7.8–23.8% of neighbourhoods in the top 5% or 10% asset-loss sets are absent from equally sized well-being-loss sets. Among mismatched neighbourhoods, mean SEFR is notably lower for those prioritised by well-being loss (0.39–0.80) than for those prioritised by asset loss (0.93–1.57). Welfare-grounded appraisal can therefore reveal overlooked vulnerability and support equitable climate adaptation.

Flooding is among the most destructive climate-related hazards globally, triggering physical shocks that cascade across interconnected environmental, social, and economic systems[1-3]. Climate change is compounding flood hazards through intensifying extreme rainfall, sea-level rise and storm surges, while growing populations and increasing concentrations of assets in flood-prone areas are expanding exposure and potential losses[4-9]. In England, approximately 6.3 million properties are presently exposed to riverine, coastal, or surface water flooding, a figure projected to reach around 8 million (one in four properties) by mid-century[10]. The systemic severity of these compound threats is epitomised by events like the summer 2007 floods, which inundated 44,600 homes and generated £3 billion in direct damage[11].

Beyond immediate physical destruction, flooding induces severe non-linear socio-economic disruptions. Direct asset damage propagates into long-term income volatility, housing instability, health deterioration, and restricted access to critical infrastructure[12,13]. Crucially, the translation of asset damage into well-being loss is highly non-linear and deeply unequal: for low-income households, a marginal asset shock consumes a vastly larger proportion of disposable income, while structural liquidity constraints restrict their adaptive capacity[14-16]. Consequently, floods force regressive trade-offs in essential spending like nutrition, healthcare, and education, prolonging recovery trajectories and widening systemic socio-economic divides[17,18]. Despite these complex dynamics, conventional flood risk assessments remain dominated by linear, direct monetary metrics like capital replacement costs[19-24], systematically obscuring the highly uneven socio-economic consequences of climate extremes.

To evaluate these uneven distributional outcomes, disaster economics increasingly relies on the concept of well-being loss[25,26]. Grounded in microeconomic welfare economics, well-being loss quantifies the total drop in consumption utility experienced during recovery, integrating direct asset destruction with cascading income shocks and reconstruction obligations[17,26]. Driven by the declining marginal utility of consumption, this metric explicitly accounts for how uniform asset shocks generate non-linear, highly asymmetrical welfare losses across income brackets[17,27]. At a global scale, transitioning from traditional asset metrics to welfare-adjusted accounting elevates estimated annual disaster costs from US$300 billion in direct damage to US$520 billion in well-being loss[26]. By shifting focus from *what is destroyed* to *how living standards are eroded*, well-being loss provides a rigorous foundation for equity-oriented flood risk appraisal.

Building on this welfare-economic perspective, socio-economic resilience describes the capacity of households or neighbourhoods to absorb and recover from physical asset losses without experiencing disproportionate well-being losses[18,28]. Unlike broader resilience measures based on multidimensional community capacities or infrastructure performance[29-32], socio-economic resilience isolates a specific welfare mechanism: the conversion of physical damage into losses in household well-being[25]. It is quantified as the ratio of direct asset loss to monetised well-being loss[26]. For this ratio, a value of one denotes parity between asset and monetised well-being losses. Values

above one indicate that well-being losses remain smaller than asset losses, reflecting a greater capacity to preserve living standards during recovery; by contrast, values below one indicate that physical damage has a disproportionately large impact on living standards.

Despite this conceptual progress, welfare-based resilience remains insufficiently integrated into spatial flood risk assessment. Many large-scale assessments combine flood-hazard models with population, income or asset data to estimate exposed people and the economic value at risk[13,33,34]. Recent large-scale, spatially detailed flood assessments increasingly incorporate poverty and social vulnerability, demonstrating that exposure alone does not capture communities' capacity to withstand and recover from flooding[35,36]. Yet flood-risk priorities remain commonly informed by asset losses, which are strongly influenced by property values. This approach can favour wealthier areas, where estimated monetary losses are larger, despite households generally having stronger financial buffers and recovery capacities[37,38]. Conversely, low-income communities may incur smaller absolute asset losses but experience greater reductions in consumption and well-being relative to their economic resources[39]. Assessments centred on aggregate exposure and asset loss can therefore overlook welfare-vulnerable communities in which physical damage translates into disproportionate well-being loss[34]. To our knowledge, no national-scale assessment has jointly quantified neighbourhood-level asset loss, monetised well-being loss and socio-economic resilience under flooding.

To address this gap, we develop a spatial framework for quantifying socio-economic flood resilience (SEFR) and apply it to all 6,791 Middle Layer Super Output Areas (MSOAs) in England, treated here as neighbourhood-scale units (Fig. 1; Methods). The framework traces how flood-induced physical damage translates into household consumption and well-being losses during recovery through three stages. First, we overlay residential building footprints with 2 m × 2 m flood-hazard maps to identify exposed dwellings and their flood depths. We then combine depth–damage relationships with local housing values to estimate direct household asset losses and associated repair expenditure. Second, we model post-flood recovery as a dynamic process in which unrepaired housing damage declines according to the recovery rate. Repair expenditure and housing-related income losses constrain household consumption during recovery. We convert the resulting consumption shortfalls into discounted utility losses and monetise them using the marginal utility of income. Third, we calculate SEFR as the ratio of direct asset loss to monetised well-being loss.

We implement the framework using nationally consistent Environment Agency flood-hazard maps for surface-water flooding (SWF) and river & sea flooding (RSF). The analysis covers four return-period classes (<30, 30–100, 100–1,000 and >1,000 years) under present-day and RCP8.5-based future climate conditions, yielding 16 flood scenarios. We estimate SEFR for neighbourhoods under each scenario, enabling consistent comparisons of how flood source, return period and climate conditions shape the spatial and socioeconomic distribution of resilience.

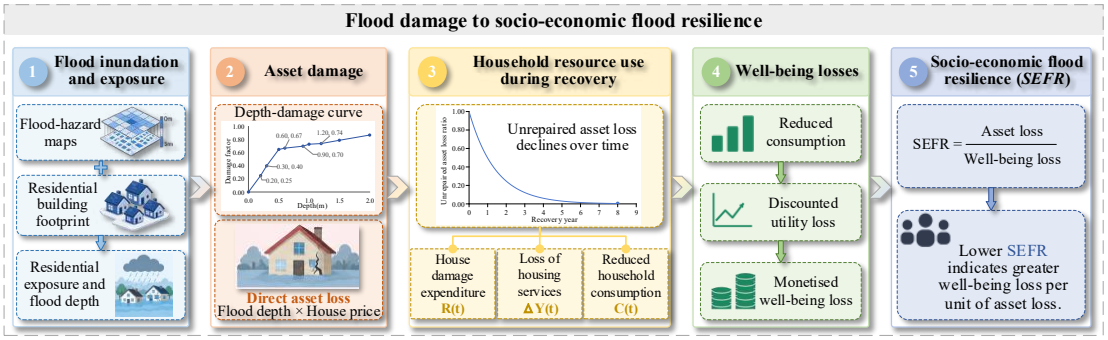


Fig. 1 | Framework for estimating household asset loss, well-being loss and SEFR.

Results

Flood severity and future climate increase losses and reduce SEFR

We estimated household asset loss, well-being loss and SEFR across 6,791 neighbourhoods (MSOAs) in England for SWF and RSF, considering four return-period classes under present-day and future RCP8.5 climate conditions. Fig. 2 illustrates the contrasting spatial patterns of residential exposure and asset loss under present-day flooding with a return period <30 years. In the example neighbourhood in Greater London, SWF produces scattered patches of inundation that intersect with residential buildings across several locations (Fig. 2a), whereas RSF inundation is concentrated in a larger, more continuous area (Fig. 2d). These differences in spatial concentration are also evident in the distribution of asset loss per household in neighbourhoods across Greater London. SWF induced losses are more widely distributed, with elevated losses across many northern and western neighbourhoods (Fig. 2b). RSF-caused losses are more localised, with relatively few neighbourhoods showing elevated losses amid extensive areas of low loss (Fig. 2e). Across England, SWF likewise produces a more geographically widespread pattern of asset loss, whereas RSF produces sharper contrasts between localised hotspots and surrounding low-loss areas (Fig. 2c,f). Together, these maps highlight how the spatial distribution of household asset loss differs between flood sources, from individual neighbourhoods to the national scale.

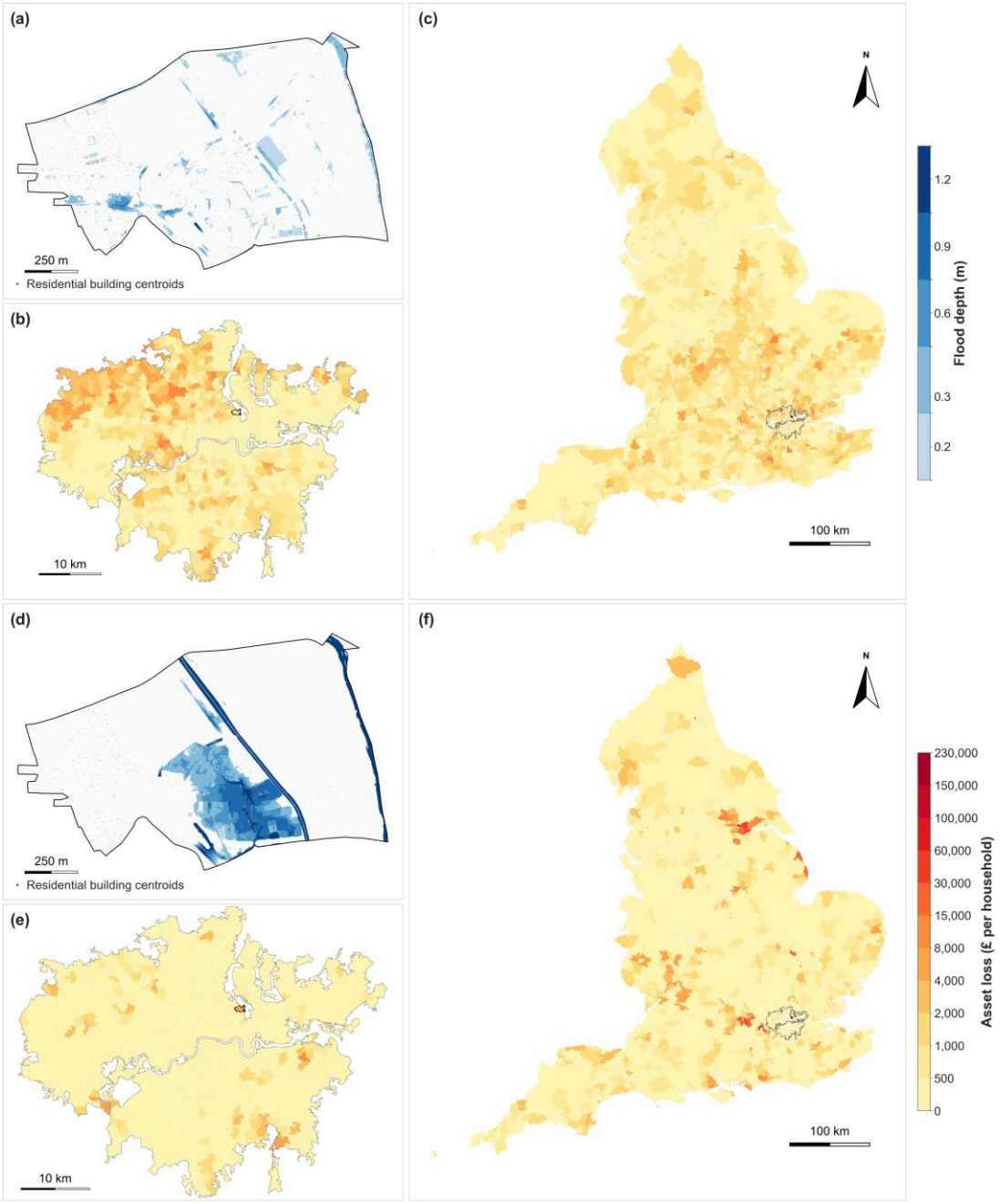


Fig. 2 | Residential flood exposure and household asset loss under present-day flooding with a return period <30 years. a, d, Residential buildings overlaid with flood depths in an example neighbourhood in Greater London under SWF and RSF, respectively; **b, e**, asset loss per household in neighbourhoods across Greater London under SWF and RSF, respectively; **c, f**, asset loss per household in neighbourhoods across England under SWF and RSF, respectively. Flood sources show contrasting spatial patterns of household asset loss, with more widespread losses under SWF and more localised losses under RSF.

Fig. 3 summarises the national distributions of household asset loss, well-being loss and SEFR among neighbourhoods. Across both flood sources, asset loss and well-being loss increase with return period, whereas SEFR declines, indicating that more severe flood events are associated with

greater physical and welfare losses and lower SEFR. Future climate conditions shift the distributions in the same direction, with higher losses and lower SEFR across all return periods. This suggests that climate change acts as a broad risk amplifier, increasing both the monetary and welfare flood burden rather than only intensifying isolated extreme events. Because SEFR captures the relationship between asset loss and monetised well-being loss, its decline should be interpreted as evidence that larger flood shocks are increasingly translated into disproportionate recovery burdens.

The distributional patterns in Fig. 3 also differ markedly by flood source. Among affected neighbourhoods, RSF exhibits broader distributions of asset loss and well-being loss, indicating greater heterogeneity across neighbourhoods. By contrast, SWF produces higher mean losses, particularly under extreme events. RSF-affected neighbourhoods also generally show higher mean SEFR than those affected by SWF. These contrasts indicate that flood source shapes not only the magnitude and variability of physical damage, but also the extent to which damage is translated into household well-being loss. SWF generates larger average loss burdens, whereas RSF produces more uneven losses across affected neighbourhoods but higher average resilience.

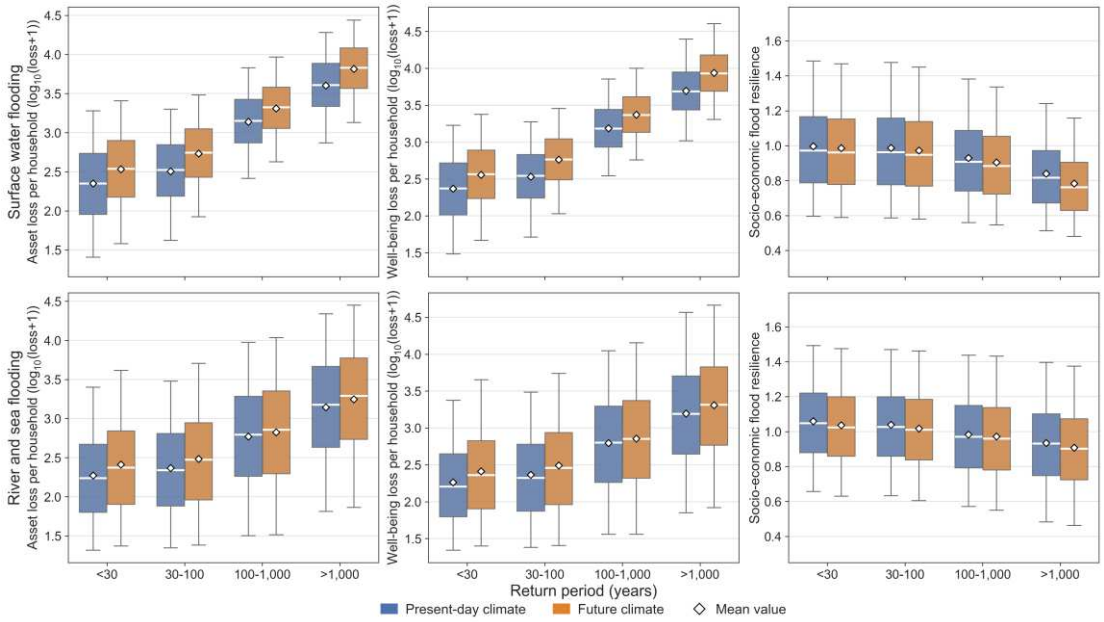


Fig. 3 | Neighbourhood-level distributions of household asset loss, monetised well-being loss and SEFR under present-day and future RCP8.5 climate conditions for SWF and RSF. Boxes span the interquartile range (25th–75th percentiles); white lines indicate medians, white diamonds indicate means, and whiskers extend to the 5th and 95th percentiles. For both flood sources, asset and well-being losses increase with return period, whereas SEFR decreases. Future climate generally shifts loss distributions upward and SEFR distributions downward, indicating that climate change increases both physical damage and the associated welfare burden while reducing SEFR.

Asset-loss rankings overlook low SEFR neighbourhoods

To assess how incorporating household well-being alters flood priorities, we ranked neighbourhoods

by asset loss and monetised well-being loss for each scenario and compared the resulting top 5% and 10% priority sets. Mismatch was defined as the proportion of asset-loss-priority neighbourhoods absent from the corresponding, equally sized well-being-loss set (Fig. 4).

Mismatch occurs in every scenario, ranging from 7.8% to 23.8% across the two selection thresholds. It is consistently greater under SWF than under RSF. Under SWF, mismatch ranges from 15.2% to 23.8% for the top 5% neighbourhoods and from 13.2% to 21.4% for the top 10% neighbourhoods; the corresponding ranges under RSF are 10.5–17.1% and 7.8–13.0%, respectively. Narrowing selection from the top 10% neighbourhoods to the top 5% neighbourhoods generally increases the mismatch, indicating that the rankings diverge even among the highest-priority neighbourhoods. Although the extent of disagreement varies with return period and climate condition, asset-loss-based selection consistently omits some neighbourhoods identified among those with the greatest well-being losses.

Among the mismatched neighbourhoods, mean SEFR ranges from 0.39 to 0.80 for those selected only by well-being loss, compared with 0.93–1.57 for those selected only by asset loss, and this separation persists across all scenarios and both selection thresholds. For present-day SWF with a return period of <30 years, the corresponding means are 0.80 and 1.57 for the top 5% selections and 0.76 and 1.51 for the top 10% selections. Because SEFR is defined as the ratio of asset loss to monetised well-being loss, the direction of this difference is expected; what is informative is its magnitude and consistency across scenarios. More importantly, incorporating well-being loss materially changes the priority set, identifying neighbourhoods with high welfare burdens that are overlooked by asset-loss-based selection.

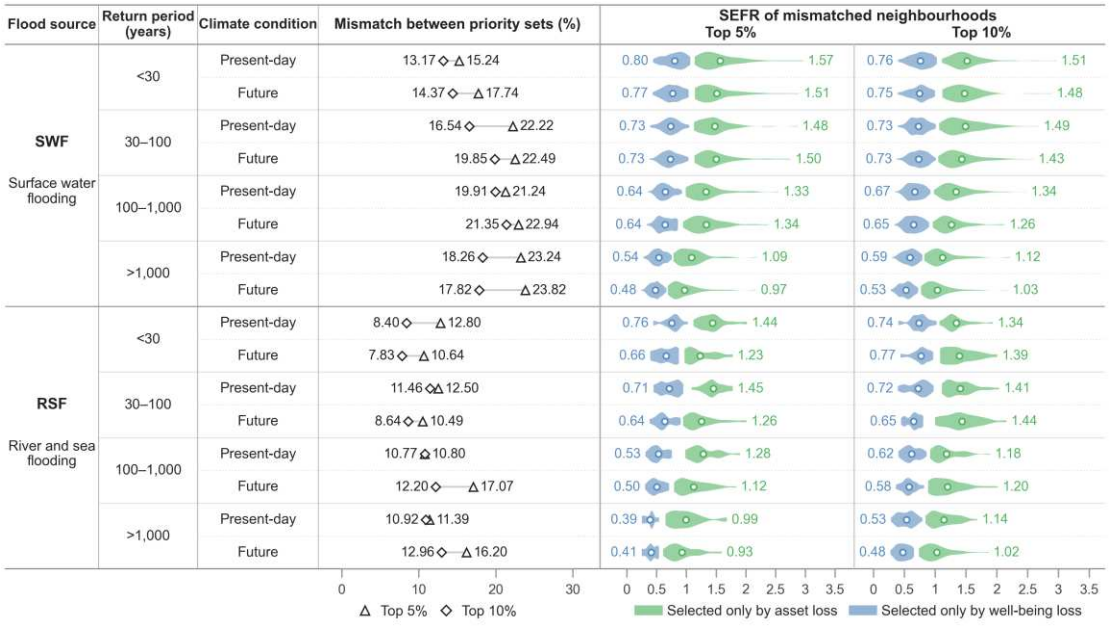


Fig. 4 | Mismatch between asset-loss and well-being-loss priorities and the resilience of mismatched neighbourhoods. Mismatch between priority sets containing the top 5% neighbourhoods or the top 10%

neighbourhoods, ranked by asset loss or monetised well-being loss. Mismatch is the percentage of asset-loss priorities absent from the equally sized well-being-loss priority set. The right panel shows SEFR distributions among mismatched neighbourhoods for the top 5% and 10% selections, respectively. White points and numerical labels indicate group means. Across all scenarios and both selection thresholds, mismatch ranges from 7.8% to 23.8%. Among the mismatched neighbourhoods, those selected only by well-being loss consistently have lower mean SEFR (0.39–0.80) than those selected only by asset loss (0.93–1.57), indicating that prioritising well-being loss identifies additional neighbourhoods with high welfare burdens and lower socio-economic resilience that asset-loss-based selection overlooks.

Low SEFR neighbourhoods are more prevalent in deprived areas

To examine how SEFR varies with neighbourhood deprivation, we assessed its association with the overall Index of Multiple Deprivation (IMD) score. Deprivation broadly refers to material and social disadvantage associated with limited resources and adverse living conditions[40]. The IMD operationalises this multidimensional concept across seven domains: income, employment, education, health and disability, crime, barriers to housing and services, and the living environment[41]. SEFR was negatively correlated with IMD across all 16 flood scenarios (Pearson's $r = -0.77$ to -0.65; all $P < 0.001$; Fig. 5). The association was similar in strength under SWF and RSF and generally weakened at higher return periods. Across both flood sources and climate conditions, correlations ranged from −0.77 to −0.76 for the two lowest return-period classes (<30 and 30–100 years), compared with −0.69 to −0.65 for return periods exceeding 1,000 years. The negative association persisted under both present-day and future climate conditions.

To quantify how the overall association translated into differences between deprivation groups, we compared SEFR distributions across IMD quintiles, from Q1 (least deprived) to Q5 (most deprived; Fig. 6). Median SEFR declined monotonically from Q1 to Q5 in every scenario under both SWF and RSF. Under present-day climate conditions and a return period of 30–100 years, median SEFR decreased from 1.27 in Q1 to 0.66 in Q5 under SWF, representing a 48.0% reduction, and from 1.27 to 0.68 under RSF, representing a 46.5% reduction. Within each quintile, median SEFR generally decreased with longer return periods and was similar or slightly lower under future climate conditions, particularly for SWF. Nevertheless, the ordering of the quintiles remained consistent across flood sources, return periods and climate conditions. Although their distributions overlapped, SEFR differed significantly across the five quintiles, and the Q1–Q5 contrast was significant in every scenario (Kruskal–Wallis and two-sided Mann–Whitney U tests, respectively; all $P<0.001$).

Together with the continuous IMD associations, these results reveal a persistent deprivation gradient in relative welfare burden: more deprived neighbourhoods experience greater monetised well-being losses per unit of asset damage. This relationship is partly expected because household income enters the SEFR calculation and income deprivation is one component of the IMD. The

quintile analysis therefore quantifies the magnitude and consistency of this distributional disparity across flood and climate scenarios, rather than establishing an independent causal effect of deprivation.

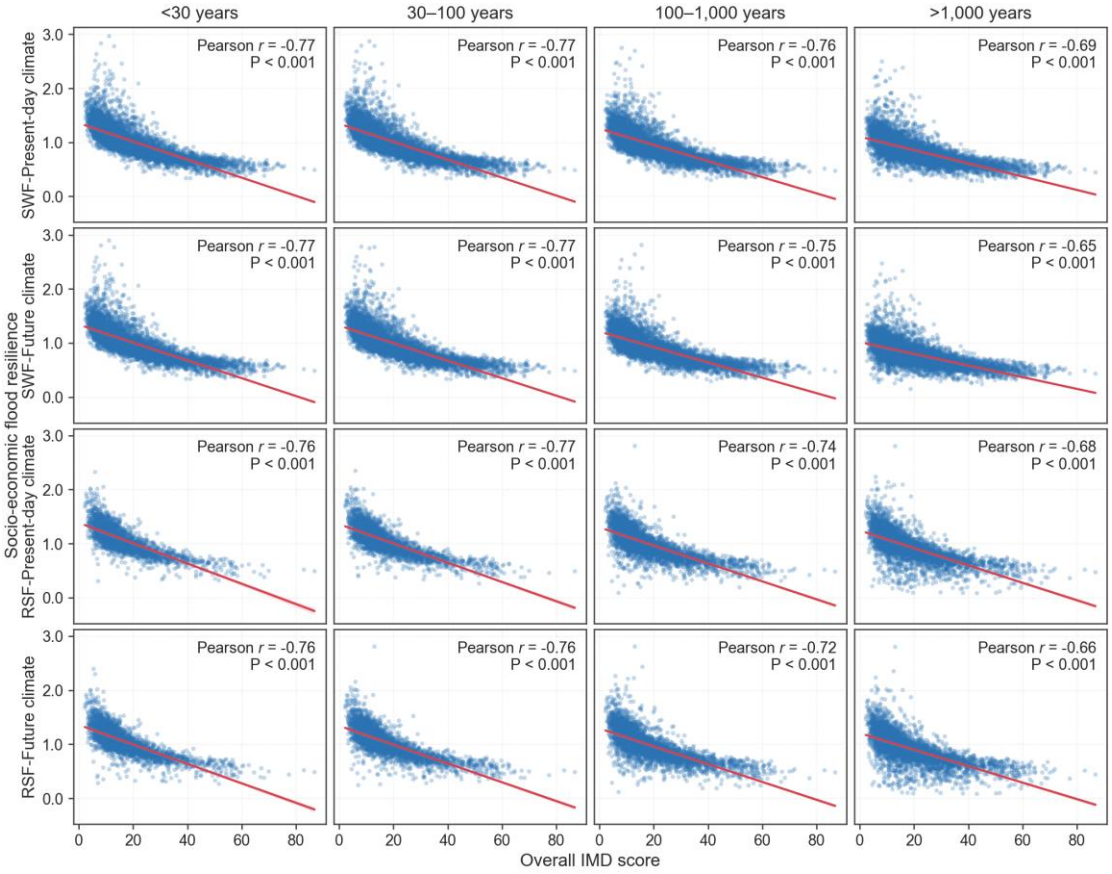


Fig. 5 | Associations between neighbourhood deprivation and SEFR across flood scenarios. Pearson's correlation coefficients and associated P values are reported in each panel. SEFR is negatively associated with deprivation across all scenarios ($r = -0.77$ to -0.65; all $P < 0.001$), with similar correlation strengths under SWF and RSF and generally weaker associations at longer return periods.

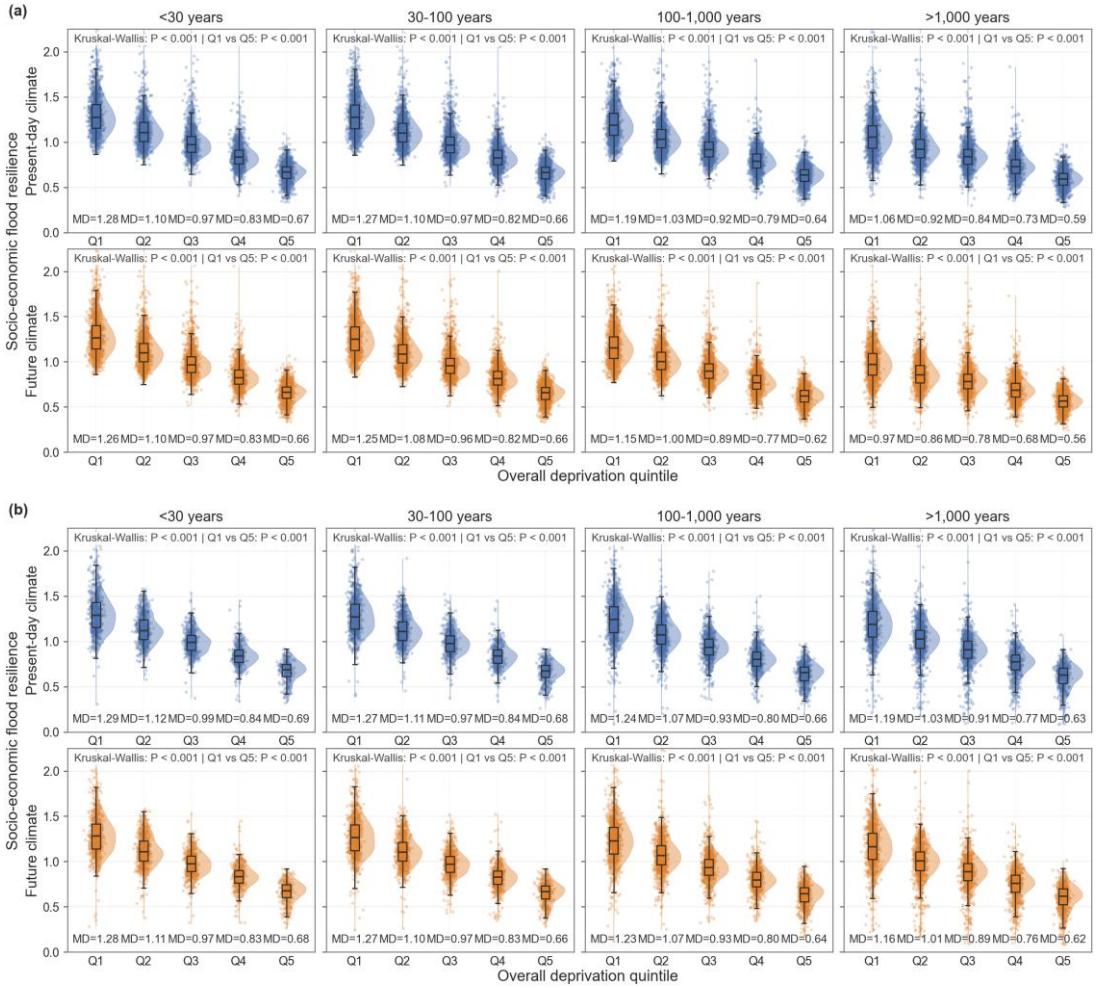


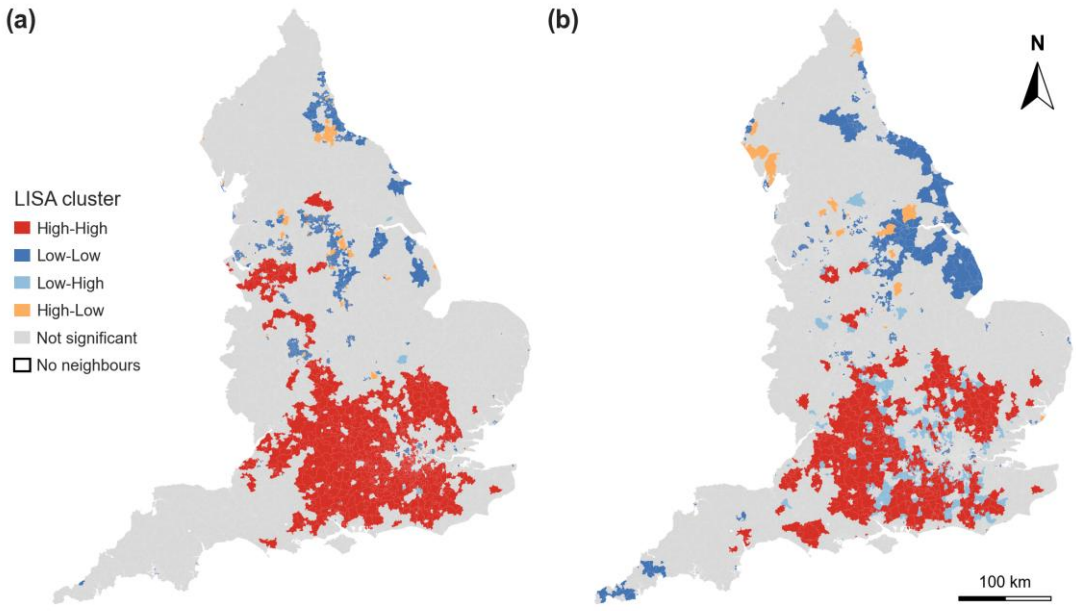
Fig. 6 | SEFR across deprivation quintiles from Q1 (least deprived) to Q5 (most deprived). Each panel shows SEFR distributions across IMD quintiles for **(a)** SWF and **(b)** RSF under different return periods and climate conditions. SEFR distributions were evaluated among affected neighbourhoods in each scenario. Points represent individual neighbourhoods, and half violins show distributions. Boxes span the 25th–75th percentiles, central lines denote medians, and whiskers extend to 1.5 times the interquartile range. MD denotes median SEFR. P values are from Kruskal–Wallis tests across all quintiles and two-sided Mann–Whitney U tests comparing Q1 with Q5. Median SEFR declines monotonically from Q1 to Q5 in all 16 scenarios, with both the overall differences and Q1–Q5 contrasts being significant in every scenario (all $P < 0.001$). This deprivation gradient persists across flood sources, return periods and climate conditions, while median SEFR generally declines towards longer return periods and under future climate conditions, particularly for SWF.

Low SEFR neighbourhoods form persistent spatial clusters across flood scenarios

SEFR exhibits clear spatial clustering across England, with neighbouring areas tending to have similar SEFR. Local Indicators of Spatial Association (LISA) identify high–high (*H–H*) and low–low (*L–L*) clusters, in which neighbourhoods and their neighbours share high or low SEFR, respectively. Under the present-day, <30-year return-period flood scenario (Fig. 7a,b), SWF-related *H–H* clusters are concentrated in southern and central England, whereas *L–L* clusters are smaller

and more dispersed across northern, central and eastern regions. Under RSF, *H–H* clusters remain concentrated in central and southern England, while *L–L* clusters are more prominent in northern, north-eastern and coastal areas, indicating a stronger regional concentration of low SEFR than under SWF.

Consistent with these local patterns, Global Moran's *I* confirms significant national-scale spatial autocorrelation across all scenarios ($P < 0.01$; Fig. 7c). SWF exhibits stronger overall clustering than RSF, with Moran's *I* ranging from 0.550 to 0.607, compared with 0.334–0.437 for RSF. Under SWF, future climate conditions slightly increase spatial dependence for a return period < 100 years but reduce it for longer return periods. For RSF, spatial clustering is stronger for rarer floods under future climate conditions. Moran's *I* increases from 0.334 for frequent floods (return period <30 years) under the present-day climate to 0.437 for very rare floods (return period >1,000 years) under future climate conditions. Future climate conditions therefore strengthen regional SEFR clustering under RSF, while reshaping rather than uniformly amplifying the already pronounced clustering under SWF.



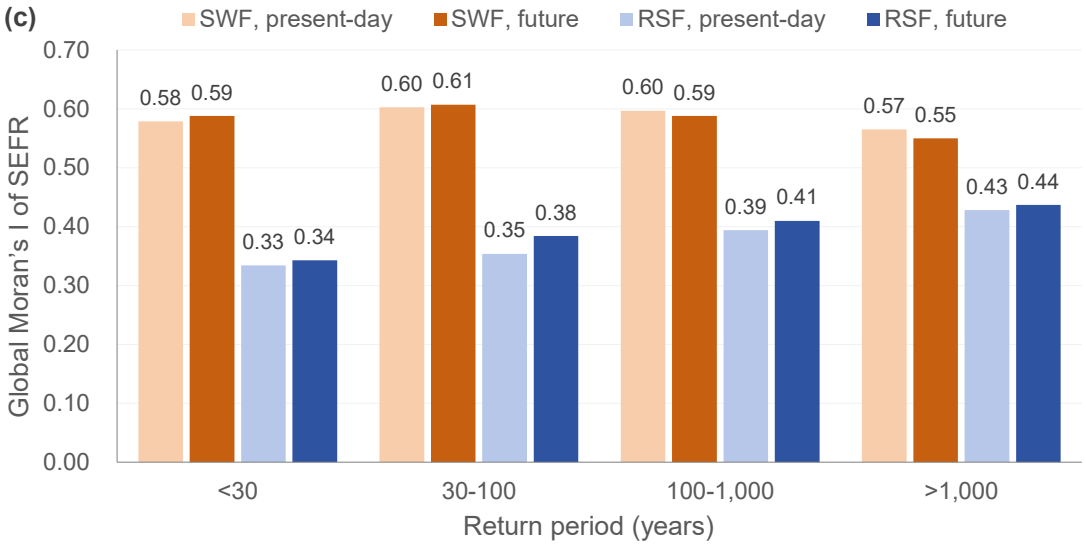


Fig. 7 | Global and local spatial autocorrelation of SEFR in England. a,b, Local Indicators of Spatial Association (LISA) clusters under present-day flooding with a return period <30 years for SWF and RSF, respectively. High–high (*H–H*) and low–low (*L–L*) denote neighbourhoods with high or low SEFR surrounded by neighbourhoods with similar values; local clusters are significant at $P < 0.05$. **c,** Global Moran's *I* coefficients for neighbourhood-level SEFR under SWF and RSF. All Moran's *I* values under different flood scenarios are positive and significant ($P < 0.01$; 999 permutations). *H–H* clusters are concentrated mainly in central and southern England, whereas *L–L* clusters are more prominent in northern, north-eastern and coastal regions. SWF exhibits stronger overall spatial autocorrelation, whereas clustering under RSF increases consistently with return period and future climate conditions.

Discussion

Flood damage induces severe, long-term consequences for household well-being that are systematically overlooked by standard asset-based metrics. Across England, evaluating consumption dynamics across the recovery trajectory uncovers stark inequalities in SEFR and could fundamentally alter adaptation priorities. While previous welfare-oriented studies on earthquakes and coastal flooding have similarly demonstrated that lower-income households suffer disproportionate welfare penalties relative to physical capital loss[17,37], our study advances this perspective by mapping these non-linear dynamics across multiple flood sources, return periods, and climate conditions.

The observed deprivation gradient in SEFR reflects the relationship between physical exposure and baseline household resources. Asset losses generally increase with household income (see Supplementary Fig. 1), while more deprived neighbourhoods generally exhibit lower SEFR at comparable asset-loss levels (see Supplementary Fig. 2). Within our framework, repair expenditures for damaged housing depress baseline consumption, generating non-linear utility losses that hit lower-income households hardest due to the diminishing marginal utility of consumption. While observational studies confirm divergent recovery trajectories across socio-economically distinct

communities facing similar physical risk[42], the observed gradient in our model aligns with structural expectations, given that income drives both SEFR and IMD. These findings quantify the magnitude of modelled welfare disparities across deprivation strata without asserting an independent causal mechanism for deprivation itself.

Accounting for household well-being changes the measured inequality of flood losses, with different effects under SWF and RSF. Under RSF, well-being losses are distributed more unequally than asset losses in every scenario. Under SWF, they are more evenly distributed in the first three return-period classes, becoming more unequal only for return periods exceeding 1,000 years (see Supplementary Fig. 3). However, the mismatch between neighbourhoods prioritised by asset loss and those prioritised by well-being loss is consistently greater under SWF than under RSF (Fig. 4). A more even distribution of well-being losses therefore does not necessarily imply closer agreement between the two priority rankings. Understanding inequality in flood impacts requires attention to both how unevenly losses are distributed and which neighbourhoods bear the greatest welfare burdens.

This distinction becomes operationally important when rankings are used to target adaptation. The persistent 7.8–23.8% mismatch between asset- and welfare-loss-based priorities among the top 5% and 10% of neighbourhoods has direct implications for adaptation targeting. Consistent with earlier vulnerability-adjusted mapping and welfare-based risk appraisals[18,35], incorporating socio-economic indicators shifts the geographic focus of risk reduction. While most priority neighbourhoods overlap between metrics, those selected exclusively by well-being loss display markedly lower mean SEFR than those chosen solely by asset loss. Notably, low SEFR does not automatically equate to the highest absolute well-being loss: the most deprived quintile does not always register the highest median well-being loss per household (see Supplementary Fig. 4). Absolute well-being loss and SEFR thus serve as complementary metrics - the former capturing welfare burden and the latter indicating the extent to which asset losses are amplified into well-being losses.

The spatial organisation of SEFR adds a further dimension to priority setting. The persistent spatial clustering of SEFR across scenarios (Fig. 7) shows that welfare vulnerability is socioeconomically patterned and geographically concentrated. This pattern reinforces the importance of spatially explicit vulnerability mapping[35]. Differences between flood sources also matter: the stronger clustering under SWF reflects the interaction of its widespread exposure pattern with regionally patterned housing values and household resources, whereas the increase in Moran's *I* for RSF under rarer events and future climate conditions indicates that regional differentiation in SEFR becomes more pronounced. Although these associations do not establish a single causal mechanism, they support coordinated, place-based adaptation and recovery strategies that address groups of nearby communities facing similar welfare and recovery constraints.

Beyond priority areas identification, robust adaptation appraisals should evaluate how

interventions alter the distribution of SEFR across communities. Evidence from flood adaptation programmes shows that benefits vary with community income and social composition[43]. Modelling of partial flood defences can reduce aggregate damage yet increase inequality in remaining losses[44]. These findings support incorporating distributional considerations into adaptation appraisal, consistent with welfare-economic approaches to flood risk management[45]. Our framework could help compare the welfare benefits of structural defences and direct recovery assistance. However, investment decisions must also consider intervention costs, engineering effectiveness and flood-event probabilities.

Future research should extend the framework to alternative socioeconomic and climate pathways, systematically propagate parameter uncertainties, and evaluate combined portfolios of adaptation interventions. Incorporating historical flood insurance claims would provide empirical validation for asset-loss estimates, while integrating household-level microdata—such as tenure type, age demographics, disability status, and credit accessibility—would uncover fine-scale vulnerabilities currently masked by spatial aggregation.

Methods

We assessed SEFR across 6,791 Middle Layer Super Output Areas (MSOAs) in England, treating each MSOA as a neighbourhood. MSOAs are census statistical areas that typically contain between 2,000 and 6,000 households[46]. For each neighbourhood and flood scenario, SEFR was calculated as the ratio of direct household asset loss to monetised well-being loss[18,28]. The assessment workflow is shown in Fig. 1.

Flood-depth maps were obtained from the Environment Agency at a spatial resolution of 2 m × 2 m[47-50] across England. The datasets cover SWF and RSF under present-day and RCP8.5-based future climate conditions, with four annual flood-likelihood classes (equivalent return periods are <30, 30–100, 100–1,000 and >1,000 years), together with five depth thresholds of 0.2, 0.3, 0.6, 0.9 and 1.2 m. Residential building footprint data, derived from Ordnance Survey (OS) OpenMap-Local, were used to identify flood-exposed dwellings within each neighbourhood. For each flood scenario, flood depth was extracted from the corresponding hazard raster at the centroid of each building footprint. These building-level depths provided the exposure inputs for estimating direct asset losses using depth–damage relationships and local housing values.

Neighbourhood-level data from 2019–2021 were used to maintain temporal and spatial consistency, as more recent data were not consistently available for all variables at the required spatial scale. Socioeconomic data included average household income, average house price and the number of households in neighbourhoods. These variables provided the socioeconomic inputs for estimating asset losses and modelling household consumption during recovery. The Index of Multiple Deprivation (IMD)[41] was used to examine differences in SEFR across deprivation levels.

IMD is the official measure of relative deprivation for small areas in England and combines seven domains: income, employment, education, health and disability, crime, barriers to housing and services, and living environment.

Asset loss estimation

This study estimates residential asset losses by integrating flood exposure, housing asset values, and depth–damage relationships. Flooded residential buildings are first identified under each flood scenario. For each exposed dwelling h located in neighbourhood i, the damage factor F_h is derived from the UK residential depth–damage function curve[51] as shown in Supplementary Fig. 5. The function is not specific to a particular flood type and is suitable for assessing generic inundation events. It is derived from a globally consistent database compiled from the literature and country-specific quantitative flood damage data. The direct asset loss is calculated as the product of the dwelling damage factor and the representative housing asset value.

To reflect the average economic burden experienced by households in each neighbourhood, the average asset loss per household in neighbourhood *i* is calculated as follows:

$$AL_i = \frac{\sum_{h \in i} P_i \cdot F_h}{N_i} \quad (1)$$

where N_i is the total number of households in neighbourhood i, which is based on the 2011 Census. P_i denotes the mean house price (£ per dwelling) in neighbourhood i, obtained from the Office for National Statistics (ONS) House Price Statistics for Small Areas (HPSSA) dataset for the year ending December 2020, and F_h represents the estimated damage factor of dwelling h associated with flood depth determined based on Supplementary Fig. S5. The term $P_i \cdot F_h$ gives a market-value-based estimate of direct residential asset loss for each exposed dwelling, and the numerator aggregates residential asset loss across all flooded dwellings in neighbourhood i.

Flood-related repair expenditures are distributed over the post-disaster recovery period rather than incurred as a one-off payment immediately after the event. To represent this dynamic recovery process, an exponential recovery model based on the framework proposed by Markhvida et al.[17] is adopted. The model assumes that the remaining unrepaired loss declines continuously over time with the progress of the repair and reconstruction work, ensuring a smooth and non-negative recovery path. The remaining unrepaired asset loss during year t after flooding is estimated as:

$$AL_i^{\text{remain}}(t) = AL_i \cdot e^{-\lambda_i t} \quad (2)$$

where $AL_i^{\text{remain}}(t)$ is the remaining unrepaired asset loss per household (£) in neighbourhood *i*. λ_i denotes the recovery rate of neighbourhood i.

The recovery process is assumed to end when 95% of the initial asset loss has been repaired [18,52]. Accordingly, the recovery duration, in years, is defined as:

$$\tau_i(\lambda_i) = \frac{-\ln(0.05)}{\lambda_i} \quad (3)$$

Based on the remaining unrepaired loss, repair expenditure $R_i(t)$ (£ per household per year) for neighbourhood i during year t is estimated as Eq. (4). This formulation captures a declining

recovery trajectory, whereby repair expenditure is highest immediately after flooding and gradually decreases as housing assets recover over time. The optimal value of λ_i for each neighbourhood is determined in the next section.

$$R_i(t) = \lambda_i \cdot AL_i^{\text{remain}}(t) \quad (4)$$

Well-being loss calculation

Beyond direct physical asset losses, flooding also generates indirect economic losses by disrupting the housing services provided by residential assets[37]. Damaged housing not only requires repair expenditure but also reduces the economic benefits households derive from their homes, commonly represented as implicit housing rents. Building upon the post-disaster recovery framework described above, income loss is estimated as a function of the remaining unrepaired housing asset loss over time.

Following the approach of Markhvida et al.[17], the housing-related income loss (£ per household per year) for neighbourhood i during year t after flooding is assumed to be proportional to the remaining unrepaired asset loss:

$$\Delta Y_i(t) = \eta \cdot AL_i^{\text{remain}}(t) \quad (5)$$

where η denotes the average productivity of housing capital. The UK economy-wide output-to-capital-stock ratio from the Penn World Table[53] is used as a proxy. For 2021, the ratio of real GDP to capital stock is approximately 0.20 for the UK. Accordingly, η is set to 20% as a proxy for housing-capital productivity in the UK context.

As this study focuses on flood-induced housing damage, the model considers the monetised loss of housing services associated with unrepaired residential assets, while other components of household income are assumed to remain unchanged. Household annual income after housing costs, denoted as Y_i, is therefore used as a proxy for pre-disaster consumption capacity in the model, which is derived from the Office for National Statistics (ONS) small area estimates of net annual household income after housing costs (equivalised) for neighbourhoods (MSOAs) in England for the financial year 2020.

$$C_{0,i} = Y_i \quad (6)$$

During the post-disaster recovery period, households face both monetised housing-service losses and repair expenditure. Household consumption in year *t* after flooding is estimated using Eq. (7), and Eq. (8) is obtained by substituting Eqs. (4) and (5) into Eq. (7). Consumption is computed as the pre-disaster consumption minus the losses due to housing-related income reductions and repair expenditure. This formulation captures the decline and recovery of household consumption after flooding, with the largest consumption losses occurring immediately after the event and gradually decreasing as housing assets recover.

$$C_i(t) = C_{0,i} - \Delta Y_i(t) - R_i(t) \quad (7)$$

$$C_i(t) = Y_i - (\eta + \lambda_i) \cdot AL_i \cdot e^{-\lambda_i t} \quad (8)$$

Building upon the dynamic consumption-loss framework above, this study further estimates

the well-being impacts of flooding by quantifying how post-disaster consumption reductions affect household welfare over time. The model follows the framework proposed by Markhvida et al. and Choong et al.[17,37], which links disaster-induced consumption losses to reductions in household well-being. Household utility at time t is represented using a constant relative risk aversion (CRRA) utility function[17]:

$$U\big(c(t)\big) = \frac{c(t)^{1-\gamma}}{1-\gamma} \tag{9}$$

where γ denotes the elasticity of marginal utility of consumption. Previous studies suggest that reasonable values of γ typically range between 0.5 and 2.0[45]. This study adopts γ =1.5 following UK-specific empirical estimates[54].

The CRRA utility function is grounded in welfare economics and is used to quantify the utility derived from a given level of consumption[37]. This model captures the diminishing marginal utility of consumption, implying that an additional unit of consumption has greater utility value for households with lower baseline consumption[18]. Accordingly, the same flood-induced consumption loss imposes a larger welfare burden on economically vulnerable households than on higher-income households. This makes the CRRA function suitable for assessing SEFR across neighbourhoods with different income levels.

Considering the temporal discounting of future utility, the cumulative well-being loss during the recovery period is estimated as the discounted utility gap between pre-disaster and post-disaster consumption trajectories:

$$\Delta U_i(\lambda_i) = \int_0^{\tau_i(\lambda_i)} \Big(U_{0,i} - U_i(t)\Big) \cdot e^{-\rho t} dt \tag{10}$$

where $\tau_i(\lambda_i)$ is the recovery duration corresponding to the optimal recovery rate λ_i. ρ represents the social discount rate, set to 3.5% following UK policy appraisal guidance[55].

In the model, the recovery rate λ_i determines how household consumption and utility change after a flood. A higher λ_i means faster reconstruction and a quicker return to the pre-flood baseline. However, it also requires greater repair spending immediately after the flood, leaving less income for consumption and reducing initial utility. Conversely, a lower λ_i preserves more consumption in the short term but delays recovery, keeping utility below the baseline for longer. Total well-being loss is measured as the area between the baseline and post-flood utility paths. The optimal recovery rate λ_i^*, therefore balances short-term consumption losses against the benefits of faster recovery and is defined as the rate that minimises cumulative discounted well-being loss shown in Eq. (11). For numerical optimisation, a small positive lower bound of $\lambda_{\min}$=0.0001 was imposed on the recovery-rate parameter to avoid evaluating the recovery process at λ_i=0.

$$\lambda_i^* = \underset{\lambda_i \in [\lambda_{\min}, \lambda_{\max,\, i}]}{\operatorname{argmin}} \Delta U_i(\lambda_i) \tag{11}$$

To ensure economically feasible recovery trajectories and avoid evaluating the CRRA utility function at zero consumption, household consumption is constrained to remain above a small

positive threshold throughout the recovery period, as shown in Eq. (12), where $C_{\min} = 10^{-6}$. Because consumption is lowest immediately after flooding, this constraint is evaluated at t=0 to derive the endogenous upper bound of the recovery rate:

$$C_i(t) > C_{\min} \tag{12}$$

$$\lambda_{\max,i}^{\text{endo}} = \frac{Y_i - C_{\min}}{AL_i} - \eta \tag{13}$$

For numerical stability, the final upper bound used in the optimisation is defined as Eq. (14). If the endogenous upper bound is non-positive or falls below $\lambda_{\min}$, no feasible positive recovery rate exists under the consumption constraint and the corresponding observation is treated as infeasible. Household flood recovery may take a few weeks to a year[56]. We conservatively set the minimum modelled time for 95% recovery at approximately one year, giving a maximum recovery rate of λ_{cap}=3.0.

$$\lambda_{\max,i} = \min(\lambda_{\text{cap}}, \lambda_{\max,i}^{\text{endo}}) \tag{14}$$

Since cumulative utility loss is measured in non-monetary utility units, it is converted into an equivalent consumption loss for easier interpretation. This conversion asks how much consumption a representative household with the benchmark income level would need to lose to experience the same well-being loss. The resulting equivalent consumption loss is interpreted as the monetised well-being loss. The utility loss is converted using the marginal utility of consumption evaluated at the common national benchmark income $\bar{Y}$ in England, defined as the household-weighted average household income after housing costs across all neighbourhoods. The monetised per-household well-being loss (£ per household) is calculated as:

$$WL_i = \frac{\Delta U_i(\lambda_i^*)}{U'(\bar{Y})} \tag{15}$$

Given the CRRA utility function, as shown in Eq. (9), $U'(c) = c^{-\gamma}$, this becomes:

$$WL_i = \frac{\Delta U_i(\lambda_i^*)}{\bar{Y}^{-\gamma}} \tag{16}$$

This process is equivalent to scaling up losses affecting poor people and scaling down losses affecting rich people, such that one unit of loss has the same impact on well-being regardless of the income of the affected household[17].

Socio-economic flood resilience

SEFR reflects the ability of households to cope with any severity of asset losses when they occur and mitigate the impact of asset losses from disasters on losses of well-being[18,28]. It can be measured as the ratio between per-household physical asset loss and monetised well-being loss. This ratio captures how strongly physical flood shock is translated into welfare impacts. For the same level of asset loss, a neighbourhood with lower well-being loss is considered more resilient, because households are better able to absorb the damage without a large reduction in consumption and welfare.

$$SEFR_i = \frac{AL_i}{WL_i} \quad (17)$$

A higher $SEFR_i$ indicates that a given level of physical asset loss results in relatively smaller well-being impacts, implying stronger SEFR. Conversely, a lower $SEFR_i$ suggests that equivalent physical losses translate into disproportionately larger welfare reductions, reflecting weaker recovery capacity and higher social vulnerability.

Data availability

The flood-hazard datasets analysed in this study were obtained from the Environment Agency through the Defra Data Services Platform. Residential building footprints and residential land-use data were obtained from Ordnance Survey and OpenStreetMap, respectively. Socioeconomic and geographic datasets, including household income, house prices, population estimates, household counts and administrative boundaries, were obtained from the Office for National Statistics, while deprivation data were obtained from the English Indices of Deprivation 2019. Detailed information on all input datasets, including their reference periods, spatial resolutions, applications and access links, is provided in Supplementary Table 1. The original third-party datasets are available from their respective providers, subject to applicable licensing conditions, and are not redistributed in the study repository.

Code availability

The Python code used for data processing, flood-loss and socio-economic flood resilience calculations, statistical and spatial analyses, and figure generation is publicly available via Zenodo at https://zenodo.org/records/22204949.

Acknowledgements

JL (Junying Liu) acknowledges support from the National Natural Science Foundation of China (No. 72374152). JL (Jie Liu) and ZX acknowledge funding from the European Union's Horizon 2020 research and innovation programme under Marie Skłodowska-Curie grant agreement (No. 101034337). JL (Jie Liu) acknowledges the support from the National Natural Science Foundation of China (No. 72501128) and the Laboratory of Computation and Analytics of Complex Management Systems (No. KKF0202402341). JW acknowledges the support from the National Natural Science Foundation of China-United Nations Environment Programme (NSFC-UNEP) No. (42561144301). RD acknowledges the support from Stanford Doerr School of Sustainability and University of Cambridge's CRASSH for the Inclusive-Ordering Initiative.

Disclaimer

The views and opinions expressed in this paper are those of the individual authors and do not

necessarily reflect those of the sponsoring organisations.

Author Contributions

JL (Jie Liu) and TW contributed to formal analysis, validation, visualisation, writing—original draft, and writing—review and editing. JL (Junying Liu), ZL, ZX, OC and RD contributed to data curation, conceptualisation, supervision, writing—original draft, and writing—review and editing. GC, JW, MH, AC, SG and IL contributed to supervision and writing—review and editing.

Competing interests

Ramit Debnath is the guest editor for the Nature special collection on *Managing cascading and non-linear climate risks*. The other authors declare no competing interests.

References

1. Jevrejeva, S., Jackson, L. P., Grinsted, A., Lincke, D. & Marzeion, B. Flood damage costs under the sea level rise with warming of 1.5 °C and 2 °C. *Environ Res Lett* **13**, 074014 https://doi.org/10.1088/1748-9326/aacc76 (2018).
2. Centre for Research on the Epidemiology of Disasters & United Nations Office for Disaster Risk Reduction. The Human Cost of Disasters An Overview of the Last 20 Years (2000–2019). 2020).
3. Zhu, Y.*, et al.* Burden of infant mortality associated with flood in 37 African countries. *Nat Commun* **15**, 10171 https://doi.org/10.1038/s41467-024-54561-y (2024).
4. Winsemius, Hessel C.*, et al.* Global drivers of future river flood risk. *Nat Clim Change* **6**, 381-385 https://doi.org/10.1038/nclimate2893 (2016).
5. Rentschler, J.*, et al.* Global evidence of rapid urban growth in flood zones since 1985. *Nature* **622**, 87-92 https://doi.org/10.1038/s41586-023-06468-9 (2023).
6. Gudmundsson, Lukas*, et al.* Globally observed trends in mean and extreme river flow attributed to climate change. *Science* **371**, 1159–1162 https://doi.org/10.1126/science.aba3996 (2021).
7. Kirezci, E.*, et al.* Projections of global-scale extreme sea levels and resulting episodic coastal flooding over the 21st Century. *Sci Rep* **10**, 11629 https://doi.org/10.1038/s41598-020-67736-6 (2020).
8. Tellman, B.*, et al.* Satellite imaging reveals increased proportion of population exposed to floods. *Nature* **596**, 80-86 https://doi.org/10.1038/s41586-021-03695-w (2021).
9. Kephart, J. L.*, et al.* Social disparities in neighborhood flood exposure in 44,698 urban neighborhoods in Latin America. *Nat Cities* **2**, 246-253 https://doi.org/10.1038/s44284-025-00203-3 (2025).
10. Environment Agency. National assessment of flood and coastal erosion risk in England 2024. 2024).
11. Chatterton, John, Viavattene, Christophe, Morris, Joe, Penning-Rowsell, Edmund & Tapsell, Sue. The Costs of the Summer 2007 Floods in England. SC070039/R1 2010).
12. Hino, Miyuki & Nance, Earthea. Five ways to ensure flood-risk research helps the most vulnerable. *Nature* **595**, 27-29 https://doi.org/10.1038/d41586-021-01750-0 (2021).
13. Rogers, J. S., Maneta, M. P., Sain, S. R., Madaus, L. E. & Hacker, J. P. The role of climate and population change in global flood exposure and vulnerability. *Nat Commun* **16**, 1287 https://doi.org/10.1038/s41467-025-56654-8 (2025).

14. Finch, Christina, Emrich, Christopher T. & Cutter, Susan L. Disaster disparities and differential recovery in New Orleans. *Popul Environ* **31**, 179-202 https://doi.org/10.1007/s11111-009-0099-8 (2010).
15. Lindersson, Sara*, et al.* The wider the gap between rich and poor the higher the flood mortality. *Nat Sustain* **6**, 995-1005 https://doi.org/10.1038/s41893-023-01107-7 (2023).
16. Tselios, Vassilis & Tompkins, Emma L. What causes nations to recover from disasters? An inquiry into the role of wealth, income inequality, and social welfare provisioning. *Int J Disaster Risk Reduct* **33**, 162-180 https://doi.org/10.1016/j.ijdrr.2018.10.003 (2019).
17. Markhvida, Maryia, Walsh, Brian, Hallegatte, Stephane & Baker, Jack. Quantification of disaster impacts through household well-being losses. *Nat Sustain* **3**, 538-547 https://doi.org/10.1038/s41893-020-0508-7 (2020).
18. Walsh, Brian & Hallegatte, Stéphane. Measuring Natural Risks in the Philippines: Socioeconomic Resilience and Wellbeing Losses. *Econ Disaster Clim Change* **4**, 249-293 https://doi.org/10.1007/s41885-019-00047-x (2020).
19. Rahim, Md Adilur, Al Assi, Ayat, Mostafiz, Rubayet Bin & Friedland, Carol J. Effects of damage initiation points of depth-damage function on flood risk assessment. *npj Nat Hazards* **1**, https://doi.org/10.1038/s44304-024-00004-z (2024).
20. Duong, Trang Minh*, et al.* On detailed representation of flood defences and flow-wave coupling in coastal flood modelling. *npj Nat Hazards* **1**, https://doi.org/10.1038/s44304-024-00016-9 (2024).
21. United Nations Office for Disaster Risk Reduction. Technical guidance for monitoring and reporting on progress in achieving the global targets of the Sendai Framework for Disaster Risk Reduction. 2017).
22. Zhang, Shulei, Zhou, Liming, Liang, Hongbin, Obulkasim, Omarjan & Dai, Yongjiu. Underestimated agricultural losses due to flooding. *Sci Adv* **12**, https://doi.org/10.1126/sciadv.aed2754 (2026).
23. Gourevitch, Jesse D.*, et al.* Unpriced climate risk and the potential consequences of overvaluation in US housing markets. *Nat Clim Change* **13**, 250-257 https://doi.org/10.1038/s41558-023-01594-8 (2023).
24. Senapati, Sibananda. Vulnerability and risk in the context of flood-related disasters: A district-level study of Bihar, India. *Int J Disaster Risk Reduct* **82**, 103368 https://doi.org/10.1016/j.ijdrr.2022.103368 (2022).
25. Hallegatte, Stephane, Bangalore, Mook & Vogt-Schilb, Adrien Camille. Socioeconomic resilience multi-hazard estimates in 117 countries. 2016).
26. Hallegatte, S., Vogt-Schilb, A., Bangalore, M. & Rozenberg, J. *Unbreakable: building the resilience of the poor in the face of natural disasters*. (World Bank, 2017).
27. Middelanis, Robin, Jafino, Bramka Arga, Hill, Ruth, Nguyen, Minh & Hallegatte, Stephane. Global socio-economic resilience to natural disasters. 2025).
28. Hallegatte, Stephane, Bangalore, Mook & Vogt-Schilb, Adrien Camille. Assessing socioeconomic resilience to floods in 90 countries. (Bank W., 2016).
29. Laidlaw, S., Percival, S. & Kiriakoulakis, K. Community flood resilience factors: A community's perspective. *Int J Disaster Risk Reduct* **135**, 106051 https://doi.org/10.1016/j.ijdrr.2026.106051 (2026).
30. Mahoney, Emerson, Golan, Maureen, Kurth, Margaret, Trump, Benjamin D. & Linkov, Igor. Resilience-by-Design and Resilience-by-Intervention in supply chains for remote and indigenous

communities. *Nat Commun* **13**, https://doi.org/10.1038/s41467-022-28734-6 (2022).
31. Linkov, Igor & Trump, Benjamin D. *The Science and Practice of Resilience*. (Springer, Cham, 2019).
32. Laurien, Finn*, et al.* A typology of community flood resilience. *Reg Environ Change* **20**, https://doi.org/10.1007/s10113-020-01593-x (2020).
33. Dottori, Francesco, Mentaschi, Lorenzo, Bianchi, Alessandra, Alfieri, Lorenzo & Feyen, Luc. Cost-effective adaptation strategies to rising river flood risk in Europe. *Nat Clim Change* **13**, 196-202 https://doi.org/10.1038/s41558-022-01540-0 (2023).
34. Wing, Oliver E. J.*, et al.* Inequitable patterns of US flood risk in the Anthropocene. *Nat Clim Change* **12**, 156-162 https://doi.org/10.1038/s41558-021-01265-6 (2022).
35. Fox, S., Agyemang, F., Hawker, L. & Neal, J. Integrating social vulnerability into high-resolution global flood risk mapping. *Nat Commun* **15**, 3155 https://doi.org/10.1038/s41467-024-47394-2 (2024).
36. Rentschler, J., Salhab, M. & Jafino, B. A. Flood exposure and poverty in 188 countries. *Nat Commun* **13**, 3527 https://doi.org/10.1038/s41467-022-30727-4 (2022).
37. Choong, Jeanette J.*, et al.* Shared hazards, unequal outcomes: income-driven inequities in disaster risk. *npj Nat Hazards* **2**, 33 https://doi.org/10.1038/s44304-025-00087-2 (2025).
38. Hallegatte, Stéphane*, et al. Shock waves: Managing the impacts of climate change on poverty*. (World Bank Publications, 2016).
39. Kawasaki, Akiyuki & Shimomura, Natsumi. Accelerated widening of economic disparity due to recurrent floods. *Int J Disaster Risk Reduct* **102**, 104273 https://doi.org/10.1016/j.ijdrr.2024.104273 (2024).
40. Townsend, Peter. Deprivation. *J Soc Policy* **16**, 125-146 https://doi.org/10.1017/s0047279400020341 (1987).
41. Ministry of Housing, Communities & Local Government. The English indices of deprivation 2019. 2019).
42. Hong, B., Bonczak, B. J., Gupta, A. & Kontokosta, C. E. Measuring inequality in community resilience to natural disasters using large-scale mobility data. *Nat Commun* **12**, 1870 https://doi.org/10.1038/s41467-021-22160-w (2021).
43. Cano Pecharroman, L. & Hahn, C. Exposing disparities in flood adaptation for equitable future interventions in the USA. *Nat Commun* **15**, 8333 https://doi.org/10.1038/s41467-024-52111-0 (2024).
44. Kumar, Ashish S., Majumder, Rajarshi, Kapadia, Vivek P. & Bhatia, Udit. Partial flood defenses shift risks and amplify inequality in a core–periphery city. *Nat Cities* **2**, 835-846 https://doi.org/10.1038/s44284-025-00299-7 (2025).
45. Kind, Jarl, Botzen, W. J. Wouter & Aerts, Jeroen C. J. H. Accounting for risk aversion, income distribution and social welfare in cost-benefit analysis for flood risk management. *WIREs Clim Change* **8**, https://doi.org/10.1002/wcc.446 (2017).
46. Office for National Statistics. 2011 Census geographies.). Office for National Statistics (2011).
47. Environment Agency. Risk of Flooding from Rivers and Sea. https://environment.data.gov.uk/dataset/96ab4342-82c1-4095-87f1-0082e8d84ef1.
48. Environment Agency. Risk of Flooding from Rivers and Sea – Climate Change 1. https://environment.data.gov.uk/dataset/de4079f2-3569-45b2-8009-a00bccc520a1.
49. Environment Agency. Risk of Flooding from Surface Water.

https://environment.data.gov.uk/dataset/b5aaa28d-6eb9-460e-8d6f-43caa71fbe0e.

50. Environment Agency. Risk of Flooding from Surface Water – Climate Change 1. https://environment.data.gov.uk/dataset/e5b38de2-99b3-44ee-b10c-b244926878ef.
51. Huizinga, Jan, De Moel, Hans & Szewczyk, Wojciech. Global flood depth-damage functions: Methodology and the database with guidelines. EUR 28552 EN 2017).
52. Sauer, I. J., Walsh, B., Frieler, K., Bresch, D. N. & Otto, C. Understanding the distributional effects of recurrent floods in the Philippines. *iScience* **28**, 111733 https://doi.org/10.1016/j.isci.2024.111733 (2025).
53. Feenstra, Robert C., Inklaar, Robert & Timmer, Marcel P. The Next Generation of the Penn World Table. *Am Econ Rev* **105**, 3150-3182 https://doi.org/10.1257/aer.20130954 (2015).
54. Groom, Ben & Maddison, David. New Estimates of the Elasticity of Marginal Utility for the UK. *Environ Resour Econ* **72**, 1155-1182 https://doi.org/10.1007/s10640-018-0242-z (2019).
55. HM Treasury. The Green Book: UK government guidance on appraisal. *Function H. T. G. F.* PU3608 2026).
56. Association of British Insurers & National Flood Forum. Responding to Floods. 2025).

Supplementary Files

This is a list of supplementary files associated with this preprint. Click to download.

- Supplementaryinformation.docx